

Swing up and Stabilization Control Design for an Underactuated Rotary Inverted Pendulum System: Theory and Experiments

Xuebo Yang, *Member, IEEE*, Xiaolong Zheng

Abstract—In this paper, the swing up and stabilization control problems for a rotary inverted pendulum (RIP) system are solved via new control schemes, in which the swing up strategy is designed by using trajectory planning and inertia effect such that the pendulum can be swung to a desired position to trigger the stabilization controller, and the stabilization scheme is implemented by resorting to the nonlinear adaptive neural network (NN) control method and linear matrix inequation technique. By using Lyapunov stability theory, it can be proved that the target trajectory can be boundedly tracked by the arm section, and the pendulum section can be balanced in the up-right position with a small error. Finally, two experiment results are respectively given to show the effectiveness of the proposed swing up and stabilization methods.

Index Terms—Rotary inverted pendulum, underactuated systems, trajectory planning, adaptive NN control.

I. INTRODUCTION

THE rotary inverted pendulum (RIP) system (Fig.1) mainly consists of a pendulum section, an arm section and a DC motor. The working mechanism of the RIP system is that the arm section is driven by the DC motor with appropriate control command such that the downward pendulum section can be balanced in the up-right position. Early studies about RIP are motivated by the balance control problem of rockets launching. This is because the dynamics of the rocket during vertical take-off is similar to the one of RIP system with its pendulum section in the up-right position. To list some representative results, the authors in [1] presented a bang-bang-type state feedback control algorithm to swing up the pendulum to its up-right position, moreover, a conventional linear quadratic regulator (LQR) method was applied to maintain the pendulum in the up-right position. A novel swing up control scheme was proposed in [2] by using energy control. In [3], the authors proposed a new swing up control strategy by using Fradkov's speed-gradient method. Today, the RIP system

Manuscript received Month 7, 2017; revised Month 12, 2017; accepted Month 12, 2017. This work was supported in part by National Natural Science Foundation of China (Grant No. 61773143 and 61627901) and the Natural Science Foundation of Heilongjiang Province of China (Grant No. 2017F009).

X. Yang and X. Zheng are with the Research Institute of Intelligent Control and Systems, School of Astronautics, Harbin Institute of Technology, Harbin 150001, China (e-mail: yangxuebo@gmail.com, zxldwljs@gmail.com).

control methods have been extensively used in many fields such as spacecraft attitude control [4], biped robot balance control [5], [6], vehicle and vessel self-balanced control [7], [8], flight control [9], [10], etc.

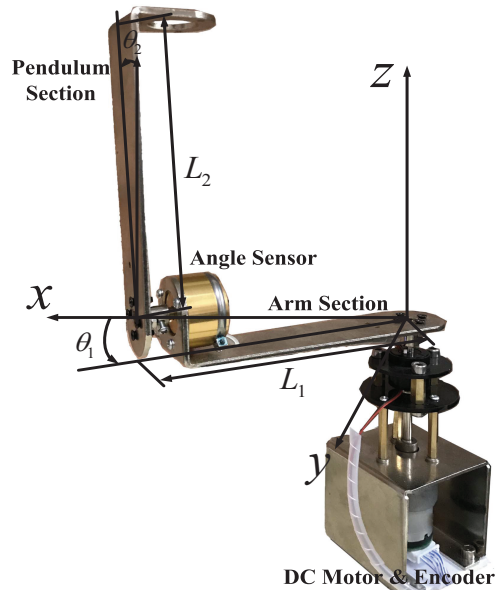


Fig. 1. The rotary inverted pendulum system.

The difficulties lie in the controller design for the RIP system are that: i) the inherent underactuated characteristic is not beneficial to the application of nonlinear control method such as backstepping technique; ii) the pendulum is unstable in its up-right position, which results in the demand for controller with high reliability and fast response speed; iii) the singularity problem occurs when the pendulum stays in the horizontal position; iv) the control performance are influenced by many factors, e.g., the system parameter uncertainties, the system itself mechanical disturbance and the external disturbance. To the best of the author's knowledge, most control methods of the RIP system consist of two steps. The first step is to design a swing up controller such that the pendulum section can be swung up to the neighborhood of the up-right position, and the second step is to maintain the pendulum section in its up-right position by using another stabilization controller. For example, in [11] and [12], the fuzzy logic control method and bang-bang control scheme were respectively used to design the

swing up controllers, and then, LQR and sliding mode control technique were applied to design stabilization controller for the RIP system.

It should be pointed out that the swing up controller design is of great importance since its performance can influence the action of the stabilization controller. However, except bang-bang control method and pseudo-state feedback [13], few other methods can be very efficient and easy to implement, which motivates us to study a new swing up strategy for the RIP system. In this note, the swing up procedure mainly takes advantage of the inertial effect of the pendulum section. First, the arm section moves back and forth to make the pendulum section have a speed, next, the arm suddenly accelerates towards a direction and then stops immediately. Due to the inertial effect, the pendulum will have an acceleration towards the same direction of the arm, which can make the pendulum exceed the horizontal position if the accelerated velocity of the arm is large enough. Although the swing up procedure is intuitively clear, the movement of the arm section needs elaborate trajectory planning and controller switching strategy, which is hard to design in terms of mathematics. Thus, to perform such a swing up procedure, practical experience and trial and error are necessary.

After completed the swing up controller design, another problem is how to design a reliable and efficient stabilization controller to maintain the balance of the pendulum. Here, it is necessary to mention that LQR is indeed a good method to stabilize the pendulum to its unstable equilibrium point (the up-right position), but such a controller only works well in a small neighborhood of the equilibrium point due to the linearization of the system model. Hence, if the swing up control fails to make the pendulum to a small neighborhood of the up-tight position, the pendulum section may be out of control, which drives us to explore a more reliable method such that the pendulum can be stabilized in the extensive region around the equilibrium point. In this paper, a nonlinear and linear controller switching scheme is proposed to stabilize the pendulum. The nonlinear controller is designed by using nonlinear uncertain system model and adaptive neural network (NN) control technique [14]–[21], whose objective is to make the pendulum rapidly swing up to a small neighborhood of the up-tight position. Then, the nonlinear RIP system model can be reduced to a linear system model with uncertainties, whose control problem can be solved via linear control theory and linear matrix inequation technique [22].

The rest of the paper is organized as follows. The RIP dynamics and its state space models are given in Section II. Swing up and stabilization controllers design is presented in Section III. Section IV shows the experimental results, and followed by Section V which concludes this paper.

II. THE RIP DYNAMICS AND ITS STATE SPACE MODELS

The rotary inverted pendulum (RIP) system shown in Fig.1 consists of six modules: a pendulum section, an arm section, a DC motor with built in gearbox ratio 20:1, a base section and two encoders as angle sensors. The symbols used are defined in Table I.

TABLE I
SYMBOLS OF THE RIP SYSTEM

Symbol	Unit	Definition
θ_1	rad	Arm angle
θ_2	rad	Pendulum angle
C_1	$\text{kg}\cdot\text{m}^2/\text{s}$	Viscous friction co-efficient of arm section
C_2	$\text{kg}\cdot\text{m}^2/\text{s}$	Viscous friction co-efficient of pendulum section
L_1	m	Physical distance between pivot of pendulum section and axis of rotation of arm section
L_2	m	Effective length of pendulum section
J_1	$\text{kg}\cdot\text{m}^2$	Moment of inertia of arm section
J_2	$\text{kg}\cdot\text{m}^2$	Moment of inertia of pendulum section
k_b	$\text{V}\cdot\text{s}/\text{rad}$	Motor back EMF constant
k_t	$\text{N}\cdot\text{m}/\text{A}$	Motor torque constant
k_u	V/count	Motor driver amplifier gain
m	kg	Effective mass of pendulum section
R	Ω	Motor armature coil resistance
g	m/s^2	Acceleration due to gravity
u	counts	Motor driving command

The Lagrangian equation of the dynamics for the rotary inverted pendulum (RIP) is in the form [23]

$$M(\theta)\ddot{\theta} + G(\theta, \dot{\theta}) + D(\theta) = \begin{bmatrix} \tau \\ 0 \end{bmatrix}, \quad (1)$$

where the elements of M , G and D matrices are given by:

$$\begin{aligned} M_{11} &= J_1 + mL_1^2 + mL_2^2 \sin^2 \theta_2, \\ M_{12} &= M_{21} = -mL_1 L_2 \cos \theta_2, \\ M_{22} &= J_2 + mL_2^2, \\ G_{11} &= C_1 + \frac{1}{2}mL_2^2 \dot{\theta}_2 \sin 2\theta_2, \\ G_{12} &= mL_1 L_2 \dot{\theta}_2 \sin \theta_2 + \frac{1}{2}mL_2^2 \dot{\theta}_1 \sin 2\theta_2, \\ G_{21} &= -\frac{1}{2}mL_2^2 \dot{\theta}_1 \sin 2\theta_2, \\ G_{22} &= C_2, D_1 = 0, D_2 = mgL_2 \sin \theta_2. \end{aligned} \quad (2)$$

The DC motor in our RIP system is controlled by using the pulse width modulation (PWM) technique, and the motor torque τ in (1) can be derived by

$$\tau = \frac{k_t k_u}{R} u - \frac{k_t k_b}{R} \dot{\theta}_1, \quad (3)$$

where k_u (V/count) is the gain of the PWM amplifier, k_t ($\text{N}\cdot\text{m}/\text{A}$) represents the motor torque constant, k_b ($\text{V}\cdot\text{s}/\text{rad}$) stands for the motor back electric motive force (EMF) constant, R (Ω) is the motor armature coil resistance, and u (count) denotes the motor driving command.

From (1)-(3), the rotary inverted pendulum dynamic model can be described by the following equations:

$$\begin{aligned} \frac{k_t k_u}{R_a} u &= (J_1 + mL_1^2 + mL_2^2 \sin^2 \theta_2) \ddot{\theta}_1 - (mL_1 L_2 \cos \theta_2) \ddot{\theta}_2 \\ &\quad + \left(C_1 + \frac{k_t k_b}{R_a} + \frac{1}{2} mL_2^2 \dot{\theta}_2 \sin 2\theta_2 \right) \dot{\theta}_1 \\ &\quad + \left(mL_1 L_2 \dot{\theta}_2 \sin \theta_2 + \frac{1}{2} mL_2^2 \dot{\theta}_1 \sin 2\theta_2 \right), \\ 0 &= -(mL_1 L_2 \cos \theta_2) \ddot{\theta}_1 + (J_2 + mL_2^2) \ddot{\theta}_2 \\ &\quad - \frac{1}{2} mL_2^2 \dot{\theta}_1^2 \sin 2\theta_2 + C_2 \dot{\theta}_2 - mgL_2 \sin \theta_2. \end{aligned} \quad (4)$$

Let $x_1 = \theta_2, x_2 = \dot{\theta}_2, x_3 = \theta_1, x_4 = \dot{\theta}_1$, it is not hard to get the following state space description in nonlinear form

$$\begin{aligned} \dot{x}_1 &= x_2, \\ \dot{x}_2 &= g_1(x)u + f_1(x) + d_c(t), \\ \dot{x}_3 &= x_4, \\ \dot{x}_4 &= g_2(x)u + f_2(x) + d_e(t), \end{aligned} \quad (5)$$

where $d_c(t)$ and $d_e(t)$ represent the combination of the RIP system itself mechanical disturbance and external disturbance in pendulum section and arm section, respectively. $g_1(x), f_1(x), g_2(x)$ and $f_2(x)$ are defined by

$$\begin{aligned} g_1(x) &= \frac{mL_1 L_2 \cos x_1}{J_2 + mL_2^2} g_2(x), \\ f_1(x) &= \frac{mL_1 L_2 \cos x_1}{J_2 + mL_2^2} f_2(x) + \frac{1}{J_2 + mL_2^2} \left(\frac{1}{2} mL_2^2 x_4^2 \sin 2x_1 \right. \\ &\quad \left. - C_2 x_2 + mgL_2 \sin x_1 \right), \\ g_2(x) &= \frac{k_t k_u}{R} \left(J_1 + mL_1^2 + mL_2^2 \sin^2 x_1 \right. \\ &\quad \left. - \frac{m^2 L_1^2 L_2^2 \cos^2 x_1}{J_2 + mL_2^2} \right)^{-1}, \\ f_2(x) &= \left(J_1 + mL_1^2 + mL_2^2 \sin^2 x_1 - \frac{m^2 L_1^2 L_2^2 \cos^2 x_1}{J_2 + mL_2^2} \right)^{-1} \\ &\quad \times \left\{ - \left(C_1 + \frac{k_t k_b}{R} + \frac{1}{2} mL_2^2 x_2 \sin 2x_1 \right. \right. \\ &\quad \left. \left. - \frac{m^2 L_1 L_2^2 x_4 \cos x_1 \sin 2x_1}{2(J_2 + mL_2^2)} \right) x_4 \right. \\ &\quad \left. - \left(mL_1 L_2 x_2 \sin x_1 + \frac{1}{2} mL_2^2 x_4 \sin 2x_1 \right. \right. \\ &\quad \left. \left. + \frac{C_2 m L_1 L_2 \cos x_1}{J_2 + mL_2^2} \right) x_2 + \frac{m^2 g L_1 L_2^2 \cos x_1 \sin x_1}{J_2 + mL_2^2} \right\}. \end{aligned} \quad (6)$$

On the other hand, system (4) can be reduced to a linear model via Taylor expansion as $x_1, x_2 \rightarrow 0$, which is given by

$$\dot{x} = (A + \Delta A)x + (B + \Delta B)u + D, \quad (7)$$

where ΔA and ΔB stand for the linear system modeling uncertainties, and

$$\begin{aligned} A &= \frac{1}{af - c^2} \begin{bmatrix} 0 & af - c^2 & 0 & 0 \\ ah & -aC_2 & 0 & -cd \\ 0 & 0 & 0 & af - c^2 \\ ch & -cC_2 & 0 & -df \end{bmatrix}, \\ B &= \frac{1}{af - c^2} [0 \ ce \ 0 \ ef]^T, D = [0, d_c(t), 0, d_e(t)]^T, \\ a &= J_1 + mL_1^2, b = mL_2^2, c = mL_1 L_2, d = C_1 + \frac{k_t k_b}{R}, \\ e &= \frac{k_t k_u}{R}, f = J_2 + mL_2^2, h = mgL_2. \end{aligned} \quad (8)$$

The control objective is to design a feedback controller such that the pendulum can be balanced in the upright position. Before the design procedure starts, the following assumptions and lemma are needed.

Assumption 1: The disturbances $d_c(t)$ and $d_e(t)$ are continuous and bounded. Furthermore, it is assumed that $D^T D \leq \bar{d}$.

Assumption 2: The system modeling uncertainties ΔA and ΔB considered here are of the form

$$\begin{aligned} \Delta A &= E_1 F_1(t) H_1, F_1^T F_1 \leq I, \\ \Delta B &= E_2 F_2(t) H_2, F_2^T F_2 \leq I, \end{aligned}$$

where E_1, E_2, H_1 and H_2 are known constant real matrices; $F_1(t)$ and $F_2(t)$ are unknown matrix function with Lebesgue measurable elements.

Lemma 1: [24] For any continuous function $f(X) : \Omega \rightarrow R$, there exist $\bar{\tau} > 0$ and a RBFNN $W^T S(X)$ such that

$$f(X) = W^T S(X) + \tau(X), |\tau(X)| \leq \bar{\tau}, \quad (9)$$

where $X = [x_1, x_2, \dots, x_q]^T \in \Omega \subset R^q$ represents the NN input vector, Ω is a compact set; $W = [w_1, w_2, \dots, w_N]^T$ and $S(X) = [s_1(X), s_2(X), \dots, s_N(X)]^T$ stand for the weight vector and the basis function vector, respectively; N denotes the node number of a neural network. In this paper, the frequently-used Gaussian functions are chosen to design $s_j(X)$

$$s_j(X) = \exp \left(- \frac{(X - C_j)^T (X - C_j)}{b_j^2} \right), \quad (10)$$

where the width and the center vector of the Gaussian function are represented by b_j and $C_j = [c_{1j}, c_{2j}, \dots, c_{qj}]^T$, respectively.

III. SWING UP AND STABILIZATION CONTROLLERS DESIGN

In this section, the swing up control scheme and the stabilization controller design will be presented in subsection A and B, respectively. The objective of the swing up controller is to make the pendulum section over its horizontal position. Then, the stabilization controller will take over control such that the pendulum can be balanced in its upright position. The control block diagram of the RIP system is given in Fig. 2, in which y_{d1} and y_{d2} are two desired trajectories, u_1 including u_t and u_s represents the swing up controller, u_2 consisting of u_n and u_l stands for the stabilization controller.

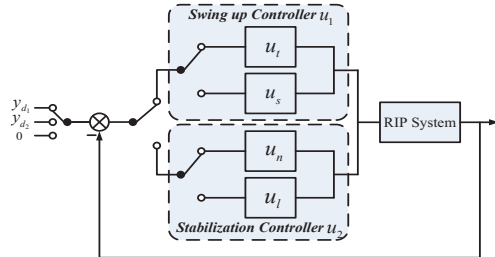


Fig. 2. The control block diagram of the RIP system.

A. Swing up controller design

This subsection is given to illustrate the swing up control scheme, which is inspired by the simple pendulum process and its inertia effect. The swing up procedure is shown in Fig. 3, which has the following three steps.

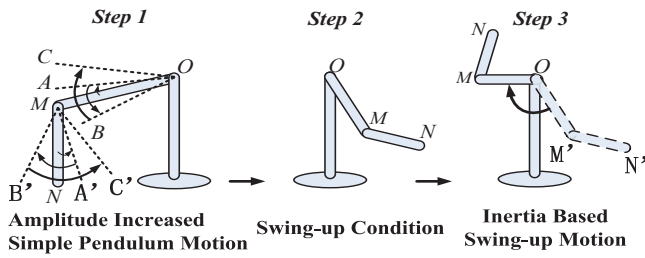


Fig. 3. Step 1. the arm section follows $OM \rightarrow OA \rightarrow OB - OC$ such that the pendulum has the motion $MN \rightarrow MA' \rightarrow MB' - MC'$; the pendulum section will trigger the swing up condition shown in step 2 as the motion amplitude increasing; then, the arm suddenly accelerates towards a direction and then stops immediately, i.e., $OM' \rightarrow OM$, which results in the motion trajectory $M'N' \rightarrow MN$ of the pendulum section.

Step 1. To perform an *amplitude increased simple pendulum motion* of the pendulum section, the arm section is designed to follow a sine-like motion which has a increasing amplitude and a decreasing period. For instance, in Fig. 3, the arm section's motion trajectory is $OM \rightarrow OA \rightarrow OB - OC$, which results in a corresponding motion trajectory $MN \rightarrow MA' \rightarrow MB' - MC'$ of the pendulum section . By trial and error, the pendulum section can start an amplitude increased simple pendulum motion if the following trajectory y_{d1} can be tracked by the arm angle x_3 .

$$y_{d1} = at \sin(bt - ct^2), \quad (11)$$

where $a = 2.9\pi \times 10^{-5}$, $b = 0.046$, $c = 2.7 \times 10^{-6}$, and Fig. 4 is given to illustrate the response of y_{d1} .

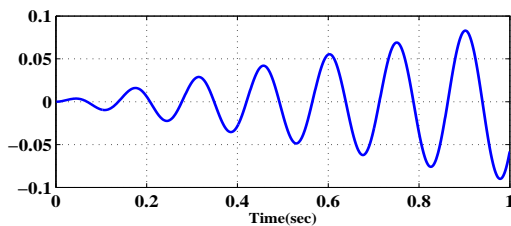


Fig. 4. The response of target trajectory y_{d1} .

In order to design the tracking controller, the following coordinate transformation is needed in the first place

$$y_1 = x_3 - y_{d1}, y_2 = x_4 - \gamma_1,$$

where $\gamma_1 = -c_1 y_1 + \dot{y}_{d1}$ with $c_1 > 0$. Let Lyapunov function $V_s = \frac{1}{2}y_1^2 + \frac{1}{2}y_2^2$, the time derivative of V_s can be given by

$$\dot{V}_s = -c_1 y_1^2 + y_1 y_2 + y_2(g_2(x)u + f_2(x) + d_e(t) - \dot{\gamma}_1). \quad (12)$$

The tracking controller $u_t = u$ can be designed as

$$u_t = -\frac{1}{g_2} \left((c_2 + 0.5)y_2 + f_2(x) + c_1 x_4 - \ddot{y}_{d1} + y_1 \right). \quad (13)$$

where $c_2 > 0$ is positive design parameter. Substituting (13) into (12), one has

$$\dot{V}_s \leq -a_0 V_s + b_0, \quad (14)$$

where $a_0 = \min\{2c_1, 2c_2\}$, $b_0 = \bar{d}/2$. Inequality (14) indicates that the desired trajectory y_{d1} can be tracked by x_3 with a bounded tracking error. As an experimental result, the pendulum section can realize an amplitude increased simple pendulum motion under the designed tracking controller u_t .

Step 2. As the amplitude of the pendulum angle increasing, the pendulum section tends to converge toward its horizontal position. Here, a *swing up condition* (see Fig. 3, the second schematic diagram) is used to start a controller switching scheme, which can be abstracted to the following equations.

$$u_1 = \begin{cases} u_t, & x_1, x_2 \notin \Omega_a, \\ u_s, & \text{otherwise,} \end{cases} \quad (15)$$

where u_1 represents the swing up controller, $\Omega_a = \{x_1, x_2 : -0.88\pi < x_1 < -0.5\pi, |x_2| < 1.5\}$ is obtained by trial and error. It should be noticed that Ω_a is not unique. u_s is an *inertia based swing up controller*, which will be given in step 3.

Step 3. When the swing up condition is satisfied, the arm section should move towards a direction at a fast speed and then stop immediately. Due to the inertial effect, the pendulum will have an acceleration towards the same direction of the arm, which can make the pendulum exceed the horizontal position if the accelerated velocity of the arm is large enough (see Fig. 3, the third schematic diagram). Such a fast movement of arm section is implemented via position control strategy, which is similar to the tracking control design in step 1. The differences between u_s and u_t is that the trajectory y_d and the values of c_1 and c_2 are changed, and u_s is given below

$$u_s = -\frac{1}{g_2} \left((c'_2 + 0.5)y_2 + f_2(x) + c_1 x_4 + y_1 \right), \quad (16)$$

where $y_1 = x_3 - y_{d2}$, $y_2 = x_4 - \gamma_2$ with $y_{d2} = -\pi$, $\gamma_2 = -c'_1 y_1$.

After the above three steps, the pendulum section can exceed its horizontal position according to our experimental results. Then, another switching scheme is given in the following such that the control right can be taken over by the stabilization controller

$$u = \begin{cases} u_1, & x_1 \notin \Omega_b, \\ u_2, & x_1 \in \Omega_b, \end{cases}$$

where $\Omega_b = \{x_1 : |x_1| \leq \pi/3\}$ is obtained by trial and error; u_2 stands for the stabilization controller, which will be designed in the next subsection.

Remark 1: The contribution of the swing up controller design is that the trajectory planning method is primarily proposed and implemented by us. Compared with bang-bang control technique [1], our method is more efficient and not limited by the small mass constraint of the pendulum section. Moreover, the motion trajectory and the switching law of the swing up controller are easy to design via one's intuition and experience. On the other hand, it should be pointed out that the parameter values used in our swing-up controllers may not be applicable for other different RIP systems. The readers should choose the corresponding values by trial and error.

B. Stabilization controller design

In this subsection, the stabilization controller is designed to balance the pendulum in its up-right position by using adaptive neural network (NN) control technique and linear control method. Before the design procedure begins, the following coordinate transformation is needed

$$z_1 = x_1, z_2 = x_2 - \alpha_1, \quad (17)$$

where $\alpha_1 = -k_1 z_1$ with $k_1 > 0$.

Theorem 1: The RIP system (4) can be stabilized by using the following nonlinear and linear switched controller

$$u_2 = \begin{cases} u_n, & x_1, x_2 \notin \Omega_c, \\ u_l, & x_1, x_2 \in \Omega_c, \end{cases}$$

with

$$\begin{aligned} u_n &= \frac{-1}{g_1(x)} \left(k_2 z_2 + f_1(x) + k_1 x_2 + z_1 + \frac{1}{2} z_2 + \frac{N}{4\eta^2} z_2 \hat{d} \right), \\ u_l &= Kx, \dot{\hat{d}} = \frac{rN}{4\eta^2} z_2^2 - \beta \hat{d}, \end{aligned}$$

where Ω_c is an appropriate set, in which linear controller u_l works well; $k_2, r, \eta, \beta > 0$ are positive constants, \hat{d} represents the approximation of $d = \|W\|^2$, K represents the feedback gain which meets the following LMI

$$\begin{bmatrix} \Xi & \bar{P}H_1^T & \bar{K}^T H_2 \\ -\varepsilon_1 I & 0 & -\varepsilon_2 I \end{bmatrix} < 0, \quad (18)$$

where ε_1 and ε_2 are positive constants and

$$\begin{aligned} \Xi &= \bar{P}A^T + A\bar{P} + \bar{K}^T B^T + B\bar{K} \\ &\quad + \varepsilon_1 E_1 E_1^T + \varepsilon_2 E_2 E_2^T + \lambda_1 I + \lambda_2 \bar{P}, \\ \bar{P} &= P^{-1}, \bar{K} = K\bar{P}, \end{aligned}$$

with P being a real positive definite symmetric matrix, λ_1 and λ_2 being positive constants.

Proof: Consider the coordinate transformation (17) and choose the Lyapunov function

$$V_a = \frac{1}{2} z_1^2 + \frac{1}{2} z_2^2 + \frac{1}{2r} \hat{d}^2,$$

where $\tilde{d} = d - \hat{d}$, $r > 0$ is a constant.

The time derivative of V_a can be given by

$$\begin{aligned} \dot{V}_a &= -k_1 z_1^2 + z_1 z_2 + z_2 \left(g_1(x)u + f_1(x) + d_c(t) - \dot{\alpha}_1 \right) - \frac{1}{r} \tilde{d} \dot{\hat{d}}, \end{aligned} \quad (19)$$

By using Lemma 1, one has

$$d_c(t) = W^T S(t) + \tau(t), |\tau(t)| \leq \bar{\tau}. \quad (20)$$

Further more, we have

$$z_2 d_c(t) \leq \frac{N}{4\eta^2} z_2^2 d + \eta^2 + \frac{1}{2} z_2^2 + \frac{1}{2} \bar{\tau}^2, \quad (21)$$

where $d = \|W\|^2$, η is a positive constant, $N > 1$ denotes the node number of a neural network,

It follows from (19) and (21) that

$$\begin{aligned} \dot{V}_a &\leq -k_1 z_1^2 + z_1 z_2 + z_2 \left(g_1(x)u + f_1(x) + k_1 x_2 + \frac{1}{2} z_2 + \frac{N}{4\eta^2} z_2 \hat{d} \right) \\ &\quad + \eta^2 + \frac{1}{2} \bar{\tau}^2 - \frac{1}{r} \tilde{d} \dot{\hat{d}}. \end{aligned} \quad (22)$$

Then, the controller $u = u_n$ and adaption law can be designed as

$$\begin{aligned} u_n &= \frac{-1}{g_1(x)} \left(k_2 z_2 + f_1(x) + k_1 x_2 + z_1 + \frac{1}{2} z_2 + \frac{N}{4\eta^2} z_2 \hat{d} \right), \\ \dot{\hat{d}} &= \frac{rN}{4\eta^2} z_2^2 - \beta \hat{d}. \end{aligned} \quad (23)$$

Substituting (23) into (22), one has

$$\begin{aligned} \dot{V}_a &\leq -k_1 z_1^2 - k_2 z_2^2 - \frac{\beta}{2r} \tilde{d}^2 + \frac{\beta}{2r} d^2 + \eta^2 + \frac{1}{2} \bar{\tau}^2 \\ &\leq -a_1 V_a + b_1, \end{aligned} \quad (24)$$

where $a_1 = \min\{2k_1, 2k_2, \beta\}$, $b_1 = \eta^2 + \frac{1}{2} \bar{\tau}^2 + \frac{\beta}{2r} d^2$. Furthermore, one has

$$V_a \leq (V_a(0) - \frac{b_1}{a_1}) e^{-a_1 t} + \frac{b_1}{a_1}. \quad (25)$$

From inequality (24), it is not hard to get that z_1 and z_2 are boundedly stable, and they will converge to a set $\Omega_1 = \{z_1, z_2 : V_a \leq \frac{b_1}{a_1}\}$ in exponential speed. Moreover, \tilde{d} will eventually converge to $\Omega_d = \{\tilde{d} : |\tilde{d}| \leq \sqrt{\frac{2rb_1}{a_1}}\}$. From the coordinate transformation in (17), one has that x_1 and x_2 will exponentially converge to a set $\Omega_2 = \{x_1, x_2 : |x_1| \leq \sqrt{\frac{2b_1}{a_1}}, |x_2| \leq (1+k_1)\sqrt{\frac{2b_1}{a_1}}\}$.

Then, system (5) can be simplified to the linear model (7), and a practical linear feedback controller $u_l = Kx$ can be designed to boundedly stabilize the linearized system via the LMI (18). The rest of the proof is given in appendix.

Remark 2: It should be pointed out that the nonlinear controller u_n is an essential part of the stabilization controller due to its bridge function for the swing up procedure and stabilization process. It should be also noticed that the linear controller u_l can only guarantee the local stability, which means that such a controller may fail to stabilize the pendulum if the pendulum section is far away from the up-right position. Therefore, the nonlinear controller u_n also serves as an auxiliary controller with regard to the linear controller u_l . On

the other hand, the parameter values used in our stabilization controllers may not be applicable for other different RIP systems. The readers should choose the corresponding values by trial and error.

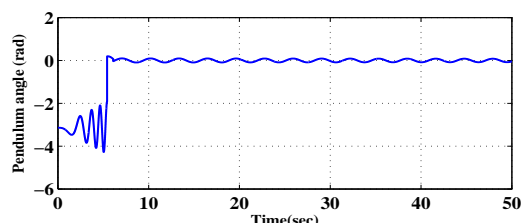
IV. SIMULATION AND EXPERIMENTAL RESULTS

A. Simulation studies

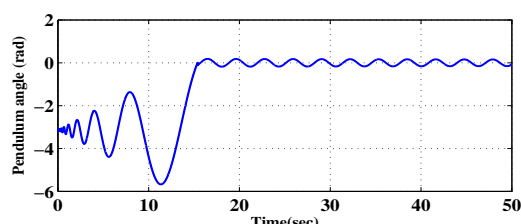
Firstly, simulation results are given by using our controller and bang-bang-LQR controller, respectively. In order to generate the disturbances, it is assumed that $d_c(t) = 0.02 \sin(0.5t)$, $d_e(t) = 0.01 \cos(0.5t)$, $E_1 = [0, 0.1, 0, 0.2]^T$, $H_1 = [0, 0.1, 0, 0.4]$, $F_1(t) = 0.1 \sin(0.5t)$, $E_2 = [0, 0.2, 0, 0.1]$, $H_2 = 0.1$, $F_2(t) = 0.05 \cos(0.5t)$. Our controller parameters are $a = 0.225$, $b = 0.04$, $c = 0.8$, $c_1 = 2$, $c_2 = 2$, $c'_1 = 8$, $c'_2 = 15$, $k_1 = k_2 = 15$, $r = 1$, $\beta = 1$, $\eta = 0.5$, $N = 3$. The linear feedback gain $K = [-428, -28, 6, 27]$, and the initial value of the adaptive law is $\hat{d}(0) = 0$. The parameters of bang-bang-LQR controller are: $u = -7200$, if $0 < x_1 \leq \pi/2, x_2 \geq 0$, $u = 7200$, if $-\pi/2 \leq x_1 \leq 0, x_2 \leq 0$, $Q = \text{diag}(100, 15, 50, 10)$, $R = 1$, $K = [-437, -15, 23, 59]$. The parameters of the RIP system are given in Table II.

TABLE II
PARAMETERS OF THE RIP SYSTEM

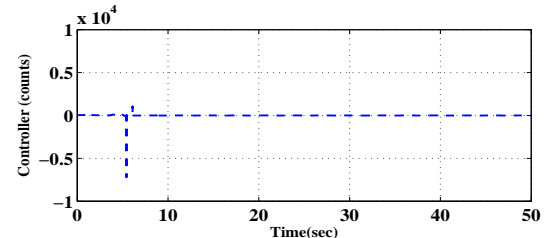
Parameter	Value	Parameter	Value
C_1	$0.025 \text{ kg}\cdot\text{m}^2/\text{s}$	k_b	$0.013 \text{ V}\cdot\text{s}/\text{rad}$
C_2	$0.001 \text{ kg}\cdot\text{m}^2/\text{s}$	k_t	$6.58 \text{ N}\cdot\text{m}/\text{A}$
L_1	0.15 m	k_u	$0.0016 \text{ V}/\text{count}$
L_2	0.135 m	m	0.152 kg
J_1	$0.0026 \text{ kg}\cdot\text{m}^2$	R	4.55Ω
J_2	$0.0014 \text{ kg}\cdot\text{m}^2$	g	9.8 m/s^2



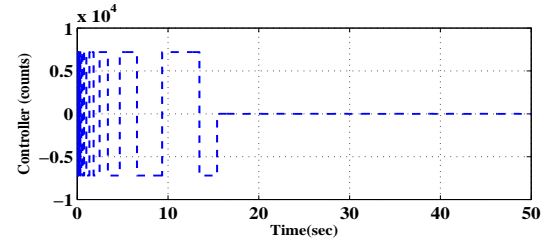
(a) Response under our controller.



(b) Response under bang-bang-LQR controller.



(c) Response of our controller.



(d) Response of bang-bang-LQR controller.

Fig. 5. Simulation results

The simulation results are shown in Fig. 5 (a)-(d). The responses of pendulum angle by respectively using our method and bang-bang-LQR technique are illustrated in Fig. 5 (a) and (b), from which, one can get that our swing up procedure is fast than the one by using bang-bang control scheme. The reason is that, in bang-bang control procedure, the pendulum section needs to follow a back and forth movement until it reaches a small neighborhood of the up-right position, such a procedure will cost a lot of time. However, in our method, the pendulum section can be swung up with less movement due to high-efficiency utilization of the inertia. Moreover, the stabilization procedure of our method is not limited by the position of the pendulum section, but LQR strategy requires that the pendulum section should be in a small neighborhood of the up-right position due to the linearization of the system model. Fig. 5 (c) and (d) demonstrate the response of the control inputs by respectively using our method and bang-bang-LQR scheme. It should be pointed out that the multiple switching of bang-bang-LQR controller may cause the damage of the motor. However, the switching frequency of our controller is quite less than the one of bang-bang-LQR controller. The detailed performance comparisons between our method and bang-bang-LQR scheme are given in Table III, in which, one can get that the swing up time, steady-state error, controller switched times and computation time of our method all are less than those of bang-bang-LQR scheme.

TABLE III
PERFORMANCE COMPARISON

	Our method	Bang-bang-LQR
Swing up time	5.4 s	15 s
Steady-state error	$\pm 0.1 \text{ rad}$	$\pm 0.2 \text{ rad}$
Controller switched times	3	37
Controller saturation time	0.005 s	13 s
Computation time	1.5 s	1.8 s

B. Experimental Results

Fig. 6 is given to show the hardware platform of the rotary inverted pendulum (RIP) system, which was made by Miniblance company. The main control chip is STM32F103, and the motor driven IC is TB6612FNG. The C language programming environment of Keil uVision-5 is used to implement the digital controller. The sampling time is set to 0.005s throughout the experiments. Our controller parameters are: $k_1 = k_2 = 3.5$, $r = 10$, $\beta = 0.1$, $\eta = 0.1$, $N = 3$. The linear feedback gain $K = [-428, -28, 6, 27]$, and the initial value of the adaptive law is $\hat{d}(0) = 0$.

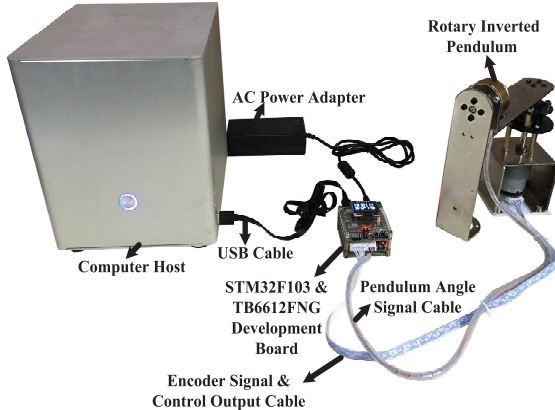
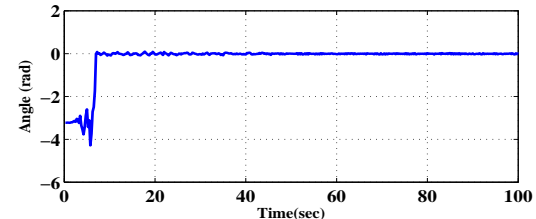


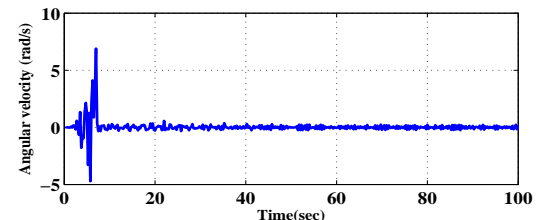
Fig. 6. The rotary inverted pendulum experimental platform.

In order to verify the effectiveness of the proposed controllers, two sets of experimental results are given in this section. The first experiment (Experiment I) is given to show the whole dynamic responses of the RIP system by using the designed swing up controller and stabilization controller under the RIP itself mechanical disturbance. The second one (Experiment II) is given to illustrate that: i) whether the stabilization controller can work well when the pendulum section's initial position stays far away from the unstable equilibrium point; ii) how is the control performance of the RIP system with external disturbance.

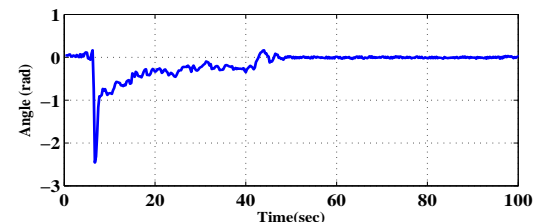
1) *Experiment I:* Experiment I demonstrates the entire process dynamic response including the swing up procedure response and the stabilization process response of the RIP system by using the designed swing up controller and stabilization controller under the RIP itself mechanical disturbance. Fig. 7 shows the captured motions of the RIP system, in which No.1-7 illustrate the amplitude increased simple pendulum motion, No.7 demonstrates the swing up condition, No.8-12 show the inertia based swing up procedure, No.13-16 depict the stabilization process.



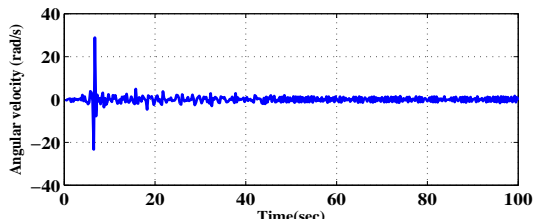
(a) Response of pendulum angle.



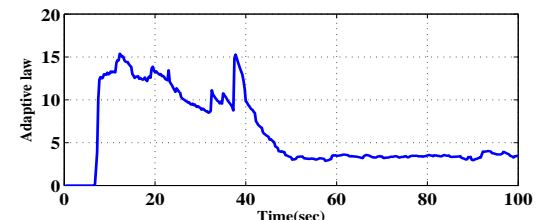
(b) Response of pendulum angle velocity.



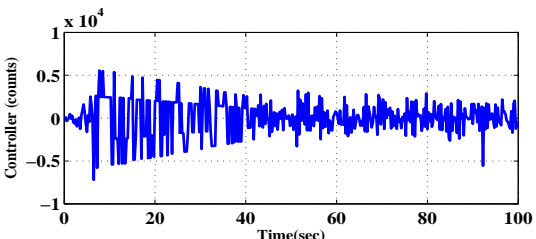
(c) Response of arm angle.



(d) Response of arm angle velocity.



(e) Response of adaptive law.



(f) Response of controller u .

Fig. 8. Responses of the RIP system signals in experiment I.

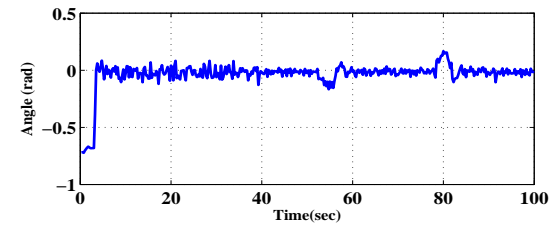


Fig. 7. The RIP swing up and stabilization procedure.

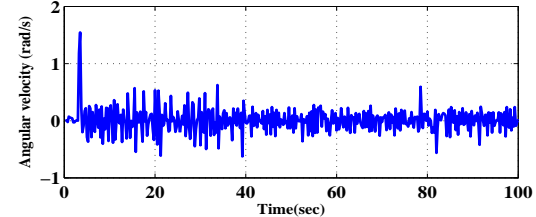
The experimental results are shown in Fig. 8 (a)-(f), respectively. Fig. 8 (a)-(d) demonstrate the responses of the pendulum angle x_1 , the pendulum angle velocity x_2 , the arm angle x_3 and the arm angle velocity x_4 , respectively. Fig. 8 (e) shows the evolution of adaptive law \hat{d} . Here, it should be noticed that the true value (d) is unknown, and \hat{d} only converges to a neighborhood of its true value, which has been proved by using (25). Fig. 8 (f) illustrates the response of controller. It can be seen in Fig. 8 (a) that the pendulum is swung up in about 7 second, and then stabilized by the stabilization controller. It is more clear from Fig. 8 (c) that the nonlinear part of the stabilization controller works from 5s to 45s, roughly. Subsequently, the linear stabilization controller takes over control after 45s. It should be noticed that all the signals of the RIP system are boundedly stable. Moreover, the swing up time, steady-state error, and controller saturation time are given numerically in Table IV.

TABLE IV
PERFORMANCE ANALYSIS

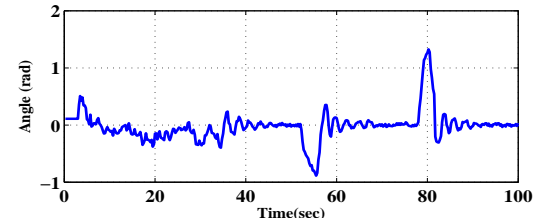
Swing up time	7 s
Steady-state error	± 0.05 rad
Controller saturation time	0.005 s



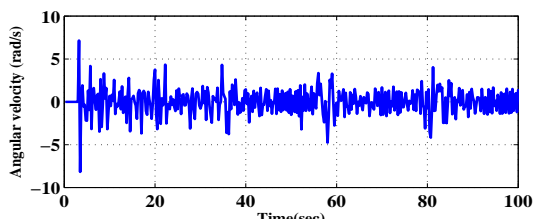
(a) Response of pendulum angle.



(b) Response of pendulum angle velocity.

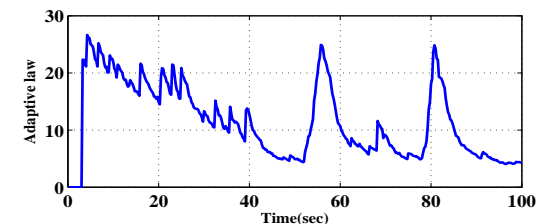


(c) Response of arm angle.

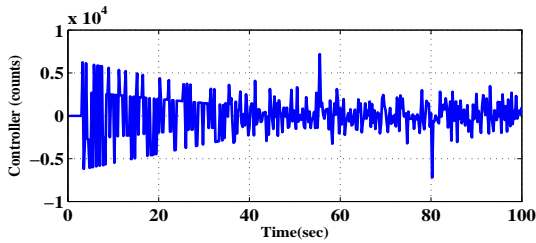


(d) Response of arm angle velocity.

2) *Experiment II:* Experiment II given here is used to illustrate that: i) whether the stabilization controller can work well when the pendulum section's initial position stays far away from the unstable equilibrium point (the initial position of the pendulum section belongs to $[-0.8, -0.6]$ rad); ii) how is the control performance of the RIP system with external disturbance. In order to generate the external disturbance, the man-made force is used to disturb the pendulum motion via pushing and pulling for 1 second respectively. It should be noticed that the swing up procedure is not used in this experiment, and the initial position of the pendulum section is set at about $[-0.8, -0.6]$ rad by hand.



(e) Response of adaptive law.



(f) Response of controller u .

Fig. 9. Responses of the RIP system signals in experiment II.

TABLE V
PERFORMANCE ANALYSIS

External force	± 2.5 N
Stabilization time	2 s
Steady-state error	± 0.05 rad
Controller saturation time	0.01 s

The experimental results are shown in Fig. 9 (a)-(f), respectively. Fig. 9 (a)-(d) demonstrate the responses of the pendulum angle x_1 , the pendulum angle velocity x_2 , the arm angle x_3 and the arm angle velocity x_4 , respectively. Fig. 9 (e) shows the evolution of adaptive law \hat{d} , and Fig. 9 (f) illustrates the response of the controller u . It can be seen in Fig. 9 (a) that the pendulum angle x_1 can be stabilized by the stabilization controller in a large initial position. Moreover, it is seen from Fig. 9 (a) and (c) that the external disturbance occurs twice at about 55s and 80s, respectively, and the stabilization controller responds rapidly to make the pendulum back to its up-right position. Table V is given to numerically show the external force, stabilization time, steady-state error and controller saturation time of our method.

TABLE VI
PERFORMANCE COMPARISON

Initial position (rad)	NLSC	SLC
$0.0 \leq x_1(0) < 0.1$	▲	▲
$0.1 \leq x_1(0) < 0.3$	▲	▲
$0.3 \leq x_1(0) < 0.6$	▲	△
$0.6 \leq x_1(0) < 0.8$	▲	△

Experiment II has shown that our stabilization controller can work well when the initial position of the pendulum

section is far away from its up-right position. In order to demonstrate the advantages of our method clear, Table VI is given to show the stability of the RIP system under different initial position by respectively using our stabilization controller (nonlinear and linear switched controller (NLSC)) and single linear controller (SLC). In Table VI, symbol “▲” represents that the RIP can be stabilized, and symbol “△” means not. From Table VI, one can see that both NLSC and SLC can work well when the initial position of the pendulum section is close to its up-right position, while SLC fails to stabilize the RIP system when the initial position is far away from the up-right position.

V. CONCLUSIONS

In this note, we have presented novel control schemes for the RIP system to swing up the pendulum and balance it in its up-right position. The swing up strategy is designed by using trajectory planning and inertia effect, and the stabilization scheme is implemented by resorting to the adaptive neural network (NN) control method and linear matrix inequation technique. Compared with bang-bang swing up controller and single linear stabilization controller, our proposed controller is more flexible and reliable. In the future, we will pay attention to more complex underactuated systems by using nonlinear and linear control schemes.

VI. APPENDIX

Choose the Lyapunov function $V_b = x^T P x$, the time derivative of V_b can be obtained by

$$\begin{aligned} \dot{V}_b &= x^T P [(A + \Delta A + (B + \Delta B)K)x + D] \\ &\quad + [x^T [(A + \Delta A + (B + \Delta B)K)^T + D^T]Px \\ &= x^T [(A + BK)^T P + P(A + BK)]x \\ &\quad + x^T [(\Delta A + \Delta BK)^T P + P(\Delta A + \Delta BK)]x \\ &\quad + x^T PD + D^T Px. \end{aligned} \quad (26)$$

By using Assumptions 1 and 2, one has

$$x^T PD + D^T Px \leq \lambda_1 x^T PP^T x + \lambda_1^{-1} \bar{d}, \quad (27)$$

$$2x^T P \Delta A x \leq \varepsilon_1 x^T PE_1 E_1^T Px + \varepsilon_1^{-1} x^T H_1^T H_1 x, \quad (28)$$

$$\begin{aligned} 2x^T P \Delta B K x &\leq \varepsilon_2 x^T PE_2 E_2^T Px \\ &\quad + \varepsilon_2^{-1} x^T K^T H_2^T H_2 K x. \end{aligned} \quad (29)$$

It follows from (26)-(29) that

$$\begin{aligned} \dot{V}_b &\leq x^T [(A + BK)^T P + P(A + BK) + \varepsilon_1 PE_1 E_1^T P \\ &\quad + \varepsilon_1^{-1} H_1^T H_1 + \varepsilon_2 PE_2 E_2^T P + \varepsilon_2^{-1} K^T H_2^T H_2 K \\ &\quad + \lambda_1 PP^T]x + \lambda_1^{-1} \bar{d}. \end{aligned} \quad (30)$$

The bounded stability can be obtained if $\dot{V}_b \leq -\lambda_2 V_b + \lambda_1^{-1} \bar{d}$ with $\lambda_2 > 0$. As a result, inequality (31) follows

$$\begin{aligned} &x^T [(A + BK)^T P + P(A + BK) + \varepsilon_1 PE_1 E_1^T P \\ &\quad + \varepsilon_1^{-1} H_1^T H_1 + \varepsilon_2 PE_2 E_2^T P + \varepsilon_2^{-1} K^T H_2^T H_2 K \\ &\quad + \lambda_1 PP^T]x + \lambda_2 x^T Px \leq 0. \end{aligned} \quad (31)$$

Therefore, it is not hard to get that the bounded stability of x can be ensured if LMI (18) holds. The proof is completed here.

REFERENCES

- [1] K. Furuta, M. Yamakita, and S. Kobayashi, "Swing up control of inverted pendulum," in *Industrial Electronics, Control and Instrumentation, 1991. Proceedings. IECON '91., 1991 International Conference on*, DOI 10.1109/IECON.1991.239008, pp. 2193–2198 vol.3, Oct. 1991.
- [2] K. Åström and K. Furuta, "Swinging up a pendulum by energy control," *Automatica*, vol. 36, no. 2, pp. 287–295, 2000.
- [3] F. Gordillo, J. A. Acosta, and J. Aracil, "A new swing-up law for the Furuta pendulum," *International Journal of Control*, vol. 76, no. 8, pp. 836–844, 2003.
- [4] H. Ashrafiou and R. S. Erwin, "Sliding mode control of underactuated multibody systems and its application to shape change control," *International Journal of Control*, vol. 81, no. 12, pp. 1849–1858, 2008.
- [5] C. Chevallereau, J. W. Grizzle, and C. L. Shih, "Asymptotically stable walking of a five-link underactuated 3-D bipedal robot," *IEEE Transactions on Robotics*, vol. 25, no. 1, pp. 37–50, 2009.
- [6] T. H. S. Li, Y. T. Su, S. H. Liu, J. J. Hu, and C. C. Chen, "Dynamic balance control for biped robot walking using sensor fusion, kalman filter, and fuzzy logic," *IEEE Transactions on Industrial Electronics*, vol. 59, no. 11, pp. 4394–4408, 2012.
- [7] H. Ashrafiou, S. Nersesov, and G. Clayton, "Trajectory tracking control of planar underactuated vehicles," *IEEE Transactions on Automatic Control*, vol. 62, no. 4, pp. 1959–1965, 2017.
- [8] F. Tu, S. S. Ge, Y. S. Choo, and C. C. Hang, "Adaptive dynamic positioning control for accommodation vessels with multiple constraints," *IET Control Theory Applications*, vol. 11, no. 3, pp. 329–340, 2017.
- [9] Y. Xu, "Multi-timescale nonlinear robust control for a miniature helicopter," *IEEE Transactions on Aerospace and Electronic Systems*, vol. 46, no. 2, pp. 656–671, 2010.
- [10] X. Huang and Y. Yan, "Saturated backstepping control of underactuated spacecraft hovering for formation flights," *IEEE Transactions on Aerospace and Electronic Systems*, 2017, doi: 10.1109/TAES.2017.2679838.
- [11] N. S. Özbek and M. Ö. Efe, "Swing up and stabilization control experiments for a rotary inverted pendulum: An educational comparison," in *2010 IEEE International Conference on Systems, Man and Cybernetics*, pp. 2226–2231, Oct. 2010.
- [12] N. J. Mathew, K. K. Rao, and N. Sivakumaran, "Swing up and stabilization control of a rotary inverted pendulum," *IFAC Proceedings Volumes*, vol. 46, no. 32, pp. 654 – 659, 2013.
- [13] K. Furuta, M. Yamakita, and S. Kobayashi, "Swing-up control of inverted pendulum using pseudo-state feedback," *Proceedings of the Institution of Mechanical Engineers, Part I: Journal of Systems and Control Engineering*, vol. 206, no. 4, pp. 263–269, 1992.
- [14] Y.-K. Choi, M.-J. Lee, S. Kim, and Y.-C. Kay, "Design and implementation of an adaptive neural-network compensator for control systems," *IEEE Transactions on Industrial Electronics*, vol. 48, no. 2, pp. 416–423, 2001.
- [15] C.-M. Lin and C.-F. Hsu, "Neural-network-based adaptive control for induction servomotor drive system," *IEEE Transactions on Industrial Electronics*, vol. 49, no. 1, pp. 115–123, 2002.
- [16] C.-M. Lin and C.-F. Hsu, "Recurrent-neural-network-based adaptive-backstepping control for induction servomotors," *IEEE Transactions on Industrial Electronics*, vol. 52, no. 6, pp. 1677–1684, 2005.
- [17] A. Rubaai, M. J. Castro-Sitiriche, M. Garuba, and L. Burge, "Implementation of artificial neural network-based tracking controller for high-performance stepper motor drives," *IEEE Transactions on Industrial Electronics*, vol. 54, no. 1, pp. 218–227, 2007.
- [18] M. Chen and S. S. Ge, "Adaptive neural output feedback control of uncertain nonlinear systems with unknown hysteresis using disturbance observer," *IEEE Transactions on Industrial Electronics*, vol. 62, no. 12, pp. 7706–7716, 2015.
- [19] S. L. Dai, M. Wang, and C. Wang, "Neural learning control of marine surface vessels with guaranteed transient tracking performance," *IEEE Transactions on Industrial Electronics*, vol. 63, no. 3, pp. 1717–1727, 2016.
- [20] Y. Song and J. Guo, "Neuro-adaptive fault-tolerant tracking control of lagrange systems pursuing targets with unknown trajectory," *IEEE Transactions on Industrial Electronics*, vol. 64, no. 5, pp. 3913–3920, 2017.
- [21] G. Wen, S. S. Ge, F. Tu, and Y. S. Choo, "Artificial potential-based adaptive H_∞ synchronized tracking control for accommodation vessel," *IEEE Transactions on Industrial Electronics*, vol. 64, no. 7, pp. 5640–5647, 2017.
- [22] S. Boyd, L. El Ghaoui, E. Feron, and V. Balakrishnan, *Linear Matrix Inequalities in System and Control Theory*. Society for Industrial and Applied Mathematics, 1994.
- [23] T. K. Chye and T. C. Sang, "Rotary inverted pendulum," *School of Electrical and Electronic Engineering, Nanyang Technological University*, 1999.
- [24] J. Park and I. W. Sandberg, "Universal approximation using radial-basis-function networks," *Neural Computation*, vol. 3, no. 2, pp. 246–257, 2008.



Xuebo Yang received the B.S. degree in automation from Northeast Forestry University, Harbin, China, in 2004, the M.S. degree in control science and engineering from Harbin Engineering University, Harbin, China, in 2007, and the Ph.D. degree in control science and engineering from Harbin Institute of Technology, Harbin, China, in 2011. He is currently an Associate Professor with the Research Institute of Intelligent Control Systems, Harbin Institute of Technology. His current research interests include robust and adaptive control theory and applications, spacecraft orbital and attitude control.



Xiaolong Zheng was born in Hubei Province, China on October 8, 1990. He received the B.S. degree in automation from Yangtze University College of Technology and Engineering, Jingzhou, China, in 2013 and the M.S. degree in control theory and control engineering from Bohai University, Jinzhou, China, in 2016. He is currently working toward the Ph.D. degree in control science and engineering with Harbin Institute of Technology, Harbin, China. His research interests include adaptive control, neural networks and their applications.